Microscopic theory of pressure effects on the energy spectra of the tunable laser crystal $Gd_3Sc_2Ga_3O_{12}:Cr^{3+}$

Ma Dong-ping
*Department of Applied Physics, Sichuan University, Chengdu 610065, People's Republic of China**
and International Centre for Materials Physics, Academia Sinica, Shenyang 110015, People's Republic of China

Zhang Ji-ping
Department of Applied Physics, Sichuan University, Chengdu 610065, People's Republic of China
(Received 2 December 2002; revised manuscript received 28 March 2003; published 25 August 2003)

In this work, a theory for shifts of energy spectra due to electron-phonon interaction (EPI) has been developed. Both the temperature-independent contributions and the temperature-dependent ones of acoustic and optical branches have been derived. The former results from the interaction between the zero-point vibration of the lattice and the localized electronic state. By means of both the theory for pressure-induced shifts (PS's) of energy spectra and the theory for shifts of energy spectra due to EPI, the ''pure electronic'' PS's and the PS's due to EPI of the R_1 line, the R_2 line, and the U band of GSGG:Cr^{3+} have been calculated, respectively. The total calculated results are in good agreement with all the experimental data. The calculated results of normal-pressure energy spectra, $g_{\parallel}(R_1)$ and $g_{\perp}(R_1)$ for GSGG:Cr^{3+} are also in good agreement with experiments. Their physical origins have been explained. It is found that the mixing degree of $|t_2^2(^3T_1)e^4T_2\rangle$ and $|t_2^3\ ^2E\rangle$ base wave functions in the wave functions of R_1 level of GSGG:Cr^{3+} is remarkable under normal pressure, and the mixing degree rapidly decreases with increasing pressure. The change of the mixing degree with pressure plays a key role for not only the pure electronic PS's of the R_1 line and the R_2 line, but also the PS's of the R_1 line and the R_2 line due to EPI. The pressure-dependent behavior of the pure electronic PS of the R_1 line (or the R_2 line) is quite different from that of the PS of the R_1 line (or the R_2 line) due to EPI. It is the combined effect of them that gives rise to the total PS of the R_1 line (or the R_2 line). At 300 K and in the range of about 15–45 kbar, the mergence and/or order reversal between $t_2^2(^3T_1)e^4T_2$ levels and $t_2^3\ ^2T_1$ levels takes place, which causes the fluctuation of the rate of PS for $t_2^2(^3T_1)e^4T_2$ (or $t_2^3\ ^2T_1$) with pressure. At 300 K, both the temperature-independent contribution to the R_1 line (or the R_2 line or the U band) from EPI and the temperature-dependent one are important, however, the temperature-independent contribution is much larger than the temperature-dependent one at 70 K.

DOI: 10.1103/PhysRevB.68.054111 PACS number(s): 78.20.Hp, 71.70.Ch, 71.70.Ej, 63.20.Mt

I. INTRODUCTION

In recent years, solid tunable lasers become more and more important. Special attention is paid to a kind of new tunable-laser crystal with intermediate crystal-field strength, such as $Gd_3Sc_2Ga_3O_{12}$(GSGG):Cr^{3+} and $Gd_3Ga_5O_{12}$(GGG):Cr^{3+}.[1–3] The typical feature of the optical spectrum for the weak crystal-field case (the average energy separation $\Delta=\{\overline{E}[t_2^2(^3T_1)e^4T_2]-\overline{E}[t_2^3\ ^2E]\}<0$) is a broad emission band from $t_2^2(^3T_1)e^4T_2$; for the strong crystal-field case ($\Delta>0$), typical features are the R_1 line, the R_2 line, and their phonon sidebands from $t_2^3\ ^2E$. Especially, for the intermediate crystal-field strength, Δ is small, and accordingly $t_2^3\ ^2E$ and $t_2^2(^3T_1)e^4T_2$ states strongly couple through spin-orbit interaction and electron-phonon interaction (EPI). Thus the emission spectrum has characteristics of both $t_2^{3\,2}E$ and $t_2^2(^3T_1)e^4T_2$, which will be quantitatively represented by the degree of the mixing of $|t_2^{3\,2}E\rangle$ and $|t_2^2(^3T_1)e^4T_2\rangle$ base wave functions for the emission state in this paper.

Because $t_2^3\ ^2E$ and $t_2^2(^3T_1)e^4T_2$ of the Cr^{3+} ion possess quite different characteristics, small changes in their wave-function mixing degree induced by fluctuations in pressure, temperature, external field, or chemical composition can lead to pronounced and unusual changes in luminescence properties, which is very important for controlling tunable laser.[1,2] Thus it is a key point to investigate the variation of their wave-function mixing degree with pressure and its microscopic mechanisms in detail.

Since 1985, on the basis of the single configuration coordinate (SCC) model, much work has been devoted to elucidating the nature of the $t_2^3\ ^2E-t_2^2(^3T_1)e^4T_2$ coupling mechanisms. Several models have been developed to describe the emission line shape and lifetime of Cr^{3+} in intermediate crystal-field systems.[4–10] For GSGG:Cr^{3+} and GGG:Cr^{3+}, Hommerich and Bray observed a dramatic change of the overall emission band shape upon increasing pressure, from a nearly structureless broad U band [the transition of $t_2^2(^3T_1)e^4T_2\rightarrow t_2^3\ ^4A_2$] to a highly structured narrow band (the transition of $t_2^3\ ^2E\rightarrow t_2^3\ ^4A_2$, which includes the R_1 line, the R_2 line, and their phonon sidebands). Moreover, they measured the pressure-induced shifts (PS's) of the R_1 line, the R_2 line, and the U band at room temperature as well as the PS of the R_1 line at 70 K for GSGG:Cr^{3+}, and calculated only the R_1-line-shift reversal with pressure for GSGG:Cr^{3+} at 70 K.[1,2]

However, there were several shortcomings in the calculations of Refs. 1 and 2: (i) The pressure effect was taken into

account phenomenologically and roughly. Namely, the energy difference between the unperturbated $t_2^3\,{}^2E$ and $t_2^2({}^3T_1)e^4T_2$ levels was assumed to increase linearly with pressure according to $\Delta_p=\Delta_0+(X_T-X_E)P$, where Δ_0 referred to the ambient pressure energy separation, X_T and X_E were the shift rates of the hypothetical unmixed $t_2^2({}^3T_1)e^4T_2$ and $t_2^3\,{}^2E$ states, and P was the pressure. In fact, the PS's of the R_1 line and the U band are obviously nonlinear. (ii) SCC model was adopted, and the effect of EPI on energy levels was only taken into account in terms of the vibrational overlap integral. We found that the model and the treatment are not adequate to calculations of PS's of levels due to EPI. (iii) The $t_2^3\,{}^2E$ levels and $t_2^2({}^3T_1)e^4T_2$ levels were treated as a degenerate level, respectively. Moreover, all the other levels were not taken into account. In fact, by using the terminology of ligand-field theory, $t_2^3\,{}^2E$ and $t_2^2({}^3T_1)e^4T_2$ of the Cr^{3+} ion are two strong-field terms. $t_2^3\,{}^2E$ has two levels with Kramers degeneracy, and $t_2^2({}^3T_1)e^4T_2$ has six levels. (iv) The calculated results of PS of the R_1 line for GSGG:Cr^{3+} at 70 K were only in rough agreement with experiment; especially, up to now, PS's of the R_1 line, the R_2 line, and the U band for GSGG:Cr^{3+} at room temperature have not been calculated and explained yet. Hence it is quite necessary to solve these problems by developing different microscopic theory. This is exactly the purpose of the present work.

This paper is organized as follows. In Sec. II, a theory for PS's of energy spectra is formulated, and a theory for shifts of energy spectra due to EPI is developed. In Sec. III, as the foundations of calculations of PS's of energy spectra, the normal-pressure energy spectra, $g_{\|}(R_1)$ and $g_{\perp}(R_1)$ of GSGG:Cr^{3+} are calculated. The "pure electronic" PS's and the PS's due to EPI of the R_1 line, the R_2 line, and the U band are calculated in Sec. IV, and their physical essentials are revealed in Sec. V. Discussion and conclusions are given in Sec. VI.

II. THEORY

The PS of the R_1 line (or the R_2 line or the U band) consists of two parts, i.e., the pure electronic PS and the PS due to EPI.

A. Pure electronic PS

When EPI is not taken into account, the pure electronic PS is calculated by a theory of PS's of energy spectra. Because the physical idea and computational method of the theory were described in detail by the previous work (e.g., see Refs. 11–17), only the expressions of B, C (Racah parameters), Dq (cubic-field parameter), K, K' (trigonal-field parameters), ζ and ζ' (spin-orbit coupling parameters) as functions of χ ($\chi=R/R_0$, where R_0 and R are the local interionic distances around Cr^{3+} at normal pressure and pressure P, respectively) are given as follows. According to the theory of PS's of energy spectra, we have

$$B/B_0=C/C_0=\Phi(\chi), \tag{1}$$

$$Dq/Dq_0=\chi^{-5}\Phi^{-4}(\chi)q_{\rm eff}/(q_{\rm eff})_0, \tag{2}$$

$$q_{\rm eff}/(q_{\rm eff})_0=\exp\{-t[\Phi^{-1}(\chi)-1]-u[\Phi^{-1}(\chi)-1]^2-\cdots\}, \tag{3}$$

where $q_{\rm eff}$ is the effective charge of a ligand ion; t and u are parameters dependent on crystal properties; we always use a subscript 0 to indicate the quantities at normal pressure, and the quantities without the subscript 0 are those under pressure P. The function $\Phi(\chi)$ is called the expansion function, which represents the expansion behavior of d-electron wave functions under pressure and plays a key role for PS's of energy spectra. Its general form is

$$\Phi(\chi)=\chi^S\exp\left[-\frac{1}{2}D_1(1-\chi)^2-\frac{1}{3}D_2(1-\chi)^3-\cdots\right], \tag{4}$$

where S, D_1, and D_2 are parameters dependent on crystal properties. Moreover, we have

$$K=K_r+K_\theta, \tag{5}$$

$$K'=K_r'+K_\theta', \tag{6}$$

where K_r and K_r' are dominant. They represent the trigonal-field parameters due to the variation in radial parts of wave functions with pressure, and their expressions are

$$K_r=\left(-\frac{1}{7}\langle A(r)\rangle_0\chi^{-3}\Phi^{-2}(\chi)-\frac{20}{189}\langle B(r)\rangle_0\chi^{-5}\Phi^{-4}(\chi)\right)\frac{q_{\rm eff}}{(q_{\rm eff})_0}, \tag{7}$$

$$K_r'=\left(\frac{1}{7}\langle A(r)\rangle_0\chi^{-3}\Phi^{-2}(\chi)-\frac{5}{63}\langle B(r)\rangle_0\chi^{-5}\Phi^{-4}(\chi)\right)\frac{q_{\rm eff}}{(q_{\rm eff})_0}, \tag{8}$$

$$\langle A(r)\rangle_0=4K_0'-3K_0, \tag{9}$$

$$\langle B(r)\rangle_0=-\frac{27}{5}(K_0'+K_0). \tag{10}$$

K_θ and K_θ' are small corrections. They represent the trigonal-field parameters due to the variation in angular parts of wave functions with pressure, and we have

$$K_\theta\cong A_1(1-\chi), \tag{11}$$

$$K_\theta'\cong A_2(1-\chi), \tag{12}$$

where A_1 and A_2 are taken as adjustable parameters. Since K and K' are small for GSGG:Cr^{3+}, in order to reduce the number of parameters, $K_0=K_0'$ and $A_1=A_2$ may be approximately taken. We have found that it is sufficient to keep the first terms of the series in Eqs. (3) and (4), because these series are rapidly convergent. Thus we only need four parameters for PS's (S, D_1, t, and A_1).

By taking into account the symmetry-restricted and central-field covalency mechanisms for the electron-wave-function expansion (the former plays a major role for PS's of ζ and ζ') and adopting a convenient and simplified form, we have

$$\zeta/\zeta_0=\zeta'/\zeta_0'=\Phi^f(\chi). \tag{13}$$

According to Refs. 11–14, the value for f may be taken as 0.6.

In order to calculate PS's of energy spectra, obviously, the relation between macroscopic quantity P and microscopic quantity $\chi=R/R_0$ is necessary. By means of the synchrotron x-ray diffraction, photoluminescence, and laser heating, the experimental P-χ_h dependence of GSGG was obtained over the range of 0–500 kbar,[18]

$$P=\left[\frac{3B_0(1-\chi_h)}{\chi_h^2}\right]\exp[\eta(1-\chi_h)], \tag{14}$$

$$\eta=1.5(B_0'-1), \tag{15}$$

where $B_0=2940$ kbar, $B_0'=2.15$, and $\chi_h=R_h/(R_0)_h=[V_h/(V_0)_h]^{1/3}$ for host. Since the ionic radius of Cr^{3+} (0.755 Å) is smaller than that of substituted Sc^{3+} (0.885 Å),[19] the size misfit causes the local compression around Cr^{3+} to be larger than the compression of the host. It is found that in order to obtain the agreement between the calculated and experimental results of PS's of the R_1 line, the R_2 line, and the U band at 300 K as well as PS of the R_1 line at 70 K for GSGG:Cr^{3+}, the ratio of the local relative volume compression around Cr^{3+} to the bulk relative volume compression should be 1.2. Namely, we have

$$1-\chi^3=1.2(1-\chi_h^3). \tag{16}$$

From Eqs. (14)–(16), the P-χ dependence has been obtained and shown in Table II.

Since the complete d^3 energy matrix in a trigonally distorted cubic field is constructed in terms of Dq, B, C, ζ, ζ', K, and K' (see Sec. III), their variations with pressure give rise to the pure electronic PS's of energy spectra, which emphasizes that EPI has not been taken into account yet.

B. PS due to EPI

The PS due to EPI is calculated by a theory for shifts of energy spectra due to EPI. In Refs. 20 and 21, we calculated the thermal shift of the R line. The theoretical improvement on Refs. 20 and 21 was made in Refs. 22 and 24. In Refs. 20–24, we treated only the temperature-dependent contribution to a level from EPI. However, the contributions to energy spectra from EPI should include both the temperature-independent part and the temperature-dependent part, and the former is much more important than the latter at low temperature. Imbusch, Yen, and Schawlow measured and calculated the isotope shifts of R lines of Cr^{3+} in ruby and MgO:Cr^{3+},[25] which demonstrated the important effect of the temperature-independent contribution of EPI. Further, its very important effect on the PS's due to EPI will be clearly shown in this work. In order to calculate both the temperature-independent part and the temperature-dependent part of contributions to energy spectra from EPI, relevant theoretical formulas have to be derived as follows.

Let us consider an interaction system of localized d-electronic states of a transition-metal ion and phonons of the lattice vibration. Its Hamiltonian is

$$H=H_{\rm latt}+H_{\rm ion}+H_{\rm int}. \tag{17}$$

The electron-phonon interaction Hamiltonian is

$$H_{\rm int}=H^{(1)}+H^{(2)}+\ \ldots, \quad H^{(1)}=\sum_{\Gamma M} C(\Gamma M)\varepsilon(\Gamma M),$$

$$H^{(2)}=\sum_{\Gamma M}\sum_{\Gamma' M'}\sum_{\Gamma'' M''} D(\Gamma M;\Gamma' M',\Gamma'' M'')\times\varepsilon(\Gamma' M')\varepsilon(\Gamma'' M''), \tag{18}$$

where Γ, Γ', and Γ'' are the irreducible representations of the point group about the central metal ion, and their trigonal components are M, M', and M'', respectively; $C(\Gamma M)$ and $D(\Gamma M;\Gamma' M',\Gamma'' M'')$ are the orbital operators of d electrons of transition-metal ions; $\varepsilon(\Gamma M)$, $\varepsilon(\Gamma' M')$, and $\varepsilon(\Gamma'' M'')$ are the phonon operators. In $H^{(2)}$, $\Gamma'\times\Gamma''=\Sigma_i\Gamma_i$, and $D(\Gamma M;\Gamma' M',\Gamma'' M'')$ transforms as the M base of the Γ representation. Generally, it is sufficient to take the first-order and second-order terms.

By taking $H_{\rm int}$ as a perturbation, the zero-order approximate wave function of the i state of the total system is

$$|i\rangle=|\psi_i^{\rm el};n_1,n_2,\ldots\ n_l,\ldots\rangle=|\psi_i^{\rm el}\rangle|n_1\rangle|n_2\rangle\ldots|n_l\rangle\ldots, \tag{19}$$

where $|\psi_i^{\rm el}\rangle$ is the localized d-electronic wave function of a transition-metal ion; n_l is the occupation number of the lth phonon state.

According to Refs. 24 and 26, we have

$$\overline{|\langle n_k|\varepsilon(\Gamma M)|n_k+1\rangle|^2}=\begin{cases}\left.\begin{matrix}\frac{16}{15}\pi k^2\ \ A(\text{longitudinal})\\ \frac{12}{15}\pi k^2\ \ A(\text{transverse})\end{matrix}\right\} & \text{for } \varepsilon(T_2x_+),\ \varepsilon(T_2x_-),\text{and } \varepsilon(T_2x_0)\\ \left.\begin{matrix}\frac{128}{15}\pi k^2\ \ A(\text{longitudinal})\\ \frac{96}{15}\pi k^2\ \ A(\text{transverse})\end{matrix}\right\} & \text{for } \varepsilon(Eu_+),\ \varepsilon(Eu_-)\end{cases}, \tag{20}$$

where $A=\hbar(n_k+1)/(32\pi M_c\omega_k)$; $\mathbf{k}$ is the wave vector; M_c is the total mass of the crystal; ω_k is the frequency; the average is made for all the directions of propagation and polarization. $\overline{|\langle n_k|\varepsilon(\Gamma M)|n_k-1\rangle|^2}$ has a similar result. For cubic or approximately cubic crystal, only E and T_2 phonons need to be considered.

According to the perturbation theory, the contribution of $H_{\rm int}$ to the energy of the i state of the total system can be written as

$$\delta E(i)=\sum_{j\neq i}\frac{|(H^{(1)})_{ij}|^2}{E_i-E_j}+(H^{(2)})_{ii}. \tag{21}$$

Obviously, $[H^{(1)}]_{ii}=0$. The terms of higher-order perturbations may be neglected.

For the contribution of EPI due to acoustic branches, by using Eq. (20), we have

$$\begin{aligned}\sum_{j\neq i}\frac{|(H^{(1)})_{ij}|^2}{E_i-E_j}&=\sum_{j;\mathbf{k},\lambda}{}'\left\{\frac{\Sigma_{\Gamma m}|\langle\psi_i^{\rm el}|C(\Gamma M)|\psi_j^{\rm el}\rangle|^2\cdot|\langle n_{\mathbf{k}\lambda}|\varepsilon(\Gamma M)|n_{\mathbf{k}\lambda}+1\rangle|^2}{E_i^{\rm el}-(E_j^{\rm el}+\hbar\omega_{\mathbf{k}\lambda})}\right.\\&\left.+\frac{\Sigma_{\Gamma M}|\langle\psi_i^{\rm el}|C(\Gamma M)|\psi_j^{\rm el}\rangle^2\cdot|\langle n_{\mathbf{k}\lambda}|\varepsilon(\Gamma M)|n_{\mathbf{k}\lambda}-1\rangle|^2}{E_i^{\rm el}-(E_j^{\rm el}-\hbar\omega_{\mathbf{k}\lambda})}\right\}\\&=\frac{\hbar}{30M_c}\sum_{j\neq i}\left\{\left[\sum_M|\langle\psi_i^{\rm el}|C(T_2M)|\psi_j^{\rm el}\rangle|^2+8\sum_M|\langle\psi_i^{\rm el}|C(EM)|\psi_j^{\rm el}\rangle|^2\right]\sum_{\mathbf{k}}\frac{k^2}{\omega_{\mathbf{k}l}}\left[\frac{n_{\mathbf{k}l}+1}{E_i^{\rm el}-E_j^{\rm el}-\hbar\omega_{\mathbf{k}l}}\right.\right.\\&\left.\left.+\frac{n_{\mathbf{k}l}}{E_i^{\rm el}-E_j^{\rm el}+\hbar\omega_{\mathbf{k}l}}\right]\right\}+\frac{\hbar}{20M_c}\sum_{j\neq i}\left\{\left[\sum_M|\langle\psi_i^{\rm el}|C(T_2M)|\psi_j^{\rm el}\rangle|^2+8\sum_M|\langle\psi_i^{\rm el}|C(EM)|\psi_j^{\rm el}\rangle|^2\right]\right.\\&\left.\times\sum_{\mathbf{k}}\frac{k^2}{\omega_{\mathbf{k}t}}\left[\frac{n_{\mathbf{k}t}+1}{E_i^{\rm el}-E_j^{\rm el}-\hbar\omega_{\mathbf{k}t}}+\frac{n_{\mathbf{k}t}}{E_i^{\rm el}-E_j^{\rm el}+\hbar\omega_{\mathbf{k}t}}\right]\right\},\end{aligned} \tag{22}$$

where the summation over λ (the label of branch) includes only acoustic branches (two branches are transverse; one, longitudinal); l represents a longitudinal branch and t represents a transverse one.

Introducing the approximation of Debye model, replacing the summation over $\mathbf{k}$ with the integration and using $\rm cm^{-1}$ unit, for the acoustic branches we can obtain

$$\begin{aligned}\sum_{j\neq i}\frac{|(H^{(1)})_{ij}|^2}{E_i-E_j}&=-\sum_{j\neq i}\left\{D_{ij}\left[T_{ij}T^2\cdot P\int_0^{T_D/T}\frac{x^3}{(e^x-1)[x^2-(T_{ij}/T)^2]}\right.\right.\\&\left.\left.\times dx+\frac{1}{2}P\int_0^{T_D}\frac{y^3}{y-T_{ij}}dy\right]\right\},\end{aligned} \tag{23}$$

$$\begin{aligned}D_{ij}=\frac{k_B^3}{60\pi^3C\rho\hbar^4}\left(\frac{1}{\nu_l^5}+\frac{3}{2\nu_t^5}\right)\left[\sum_M|\langle\psi_i^{\rm el}|C(T_2M)|\psi_j^{\rm el}\rangle|^2\right.\\\left.+8\sum_M|\langle\psi_i^{\rm el}|C(EM)|\psi_j^{\rm el}\rangle|^2\right],\end{aligned} \tag{24}$$

where k_B is the Boltzmann constant; $\hbar=h/2\pi$, h is the Planck constant; $T_D=\hbar\omega_D/k_B$ is the Debye temperature of acoustic branches; $T_{ij}=(E_i^{\rm el}-E_j^{\rm el})/k_B$; P indicates the principal value of an integral (when $|T_{ij}|<T_D$, there is a singular point in the first integral; when $0<T_{ij}<T_D$, there is a singular point in the second integral); C is the velocity of light in the vacuum; ρ is the crystal density; ν_l and ν_t are longitudinal and transverse velocities of sound, respectively; $\psi^{\rm el}$ and $E^{\rm el}$ denote the d-electronic wave function and energy, respectively.

Similarly, we can derive out the contribution to $(H^{(2)})_{ii}$ from EPI due to acoustic branches,

$$(H^{(2)})_{ii}=\langle i|H^{(2)}|i\rangle=F_{ii}\left\{T^4\int_0^{T_D/T}\frac{x^3}{e^x-1}dx+\frac{T_D^4}{8}\right\}, \tag{25}$$

$$F_{ii}=\frac{k_B^4}{60\pi^3C\rho\hbar^4}\left(\frac{1}{\nu_l^5}+\frac{3}{2\nu_t^5}\right)\sum_M\langle\psi_i^{\rm el}|D(T_2M)|\psi_i^{\rm el}\rangle. \tag{26}$$

It is found that $\Sigma_M\langle\psi_i^{\rm el}|D(EM)|\psi_i^{\rm el}\rangle$ is very much smaller than $\Sigma_M\langle\psi_i^{\rm el}|D(T_2M)|\psi_i^{\rm el}\rangle$. Thus we have neglected the former.

From Eqs. (23) and (25), we have finally obtained the contribution to i-state energy of the total system from EPI due to acoustic branches (i.e., the acoustic-branch term of i level in $\rm cm^{-1}$ unit),

$$\delta E_{\mathrm{ac}}(i)=\delta E_{\mathrm{ac},T}(i)+\delta E_{\mathrm{ac},0}(i), \tag{27}$$

$$\delta E_{\mathrm{ac},T}(i)=-\sum_{j\neq i} D_{ij}T_{ij}T^2 \times P\int_0^{T_D/T}\frac{x^3}{(e^x-1)[x^2-(T_{ij}/T)^2]}dx + F_{ii}T^4\int_0^{T_D/T}\frac{x^3}{e^x-1}dx, \tag{28}$$

$$\delta E_{\mathrm{ac},0}(i)=-\frac{1}{2}\sum_{j\neq i} D_{ij}\cdot P\int_0^{T_D}\frac{y^3}{y-T_{ij}}dy+\frac{1}{8}F_{ii}T_D^4, \tag{29}$$

where the summation over j includes all the levels, except for i level.

For optical branches, the ''single frequency model'' approximation may be made (see Ref. 22, where the effective frequency is ω_{eff}). Then, we can derive the contribution to i-state energy of the total system from EPI due to optical branches (i.e., the optical-branch term of i level in cm^{-1} unit) as

$$\delta E_{\mathrm{op}}(i)=\delta E_{\mathrm{op},T}(i)+\delta E_{\mathrm{op},0}(i), \tag{30}$$

$$\delta E_{\mathrm{op},T}(i)=\gamma_T(i)\cdot[T_D^5/T_{\mathrm{op}}]\cdot(e^{T_{\mathrm{op}}/T}-1)^{-1}, \tag{31}$$

$$\delta E_{\mathrm{op},0}(i)=\gamma_0(i)\cdot\lfloor T_D^5/T_{\mathrm{op}}\rfloor, \tag{32}$$

$$\gamma_T(i)=\frac{k_B^4}{120\pi^3C\rho\nu_s^5\hbar^4}\left[\sum_{j\neq i}\frac{\left[\sum_M|\langle\psi_i^{\mathrm{el}}|C(T_2M)|\psi_j^{\mathrm{el}}\rangle|^2+8\sum_M|\langle\psi_i^{\mathrm{el}}|C(EM)|\psi_j^{\mathrm{el}}\rangle|^2\right]}{(E_i^{\mathrm{el}}-E_j^{\mathrm{el}})^2-(\hbar\omega_{\mathrm{eff}})^2}(E_i^{\mathrm{el}}-E_j^{\mathrm{el}})+\sum_M\langle\psi_i^{\mathrm{el}}|D(T_2M)|\psi_i^{\mathrm{el}}\rangle\right], \tag{33}$$

$$\gamma_0(i)=\frac{k_B^4}{240\pi^3C\rho\nu_s^5\hbar^4}\left[\sum_{j\neq i}\frac{\left[\sum_M|\langle\psi_i^{\mathrm{el}}|C(T_2M)|\psi_j^{\mathrm{el}}\rangle|^2+8\sum_M|\langle\psi_i^{\mathrm{el}}|C(EM)|\psi_j^{\mathrm{el}}\rangle|^2\right]}{(E_i^{\mathrm{el}}-E_j^{\mathrm{el}})-(\hbar\omega_{\mathrm{eff}})}+\sum_M\langle\psi_i^{\mathrm{el}}|D(T_2M)|\psi_i^{\mathrm{el}}\rangle\right], \tag{34}$$

where $T_{\mathrm{op}}=\hbar\omega_{\mathrm{eff}}/k_B$, and ν_s is defined as $3/\nu_s^3=2/\nu_t^3+1/\nu_l^3$. T_D and ν_s in Eqs. (31)–(34) come from the sum $\Sigma_k k^2=V\omega_D^5/10\pi^2\nu_s^5$ (k is the wave vector and V is the crystal volume).[22] This is obtained by using acoustic branches and the Debye model, since the values of k and their square sum are independent of whether using optical branches or acoustic ones.

It is noteworthy that $\delta E_{\mathrm{ac},0}(i)$ and $\delta E_{\mathrm{op},0}(i)$ are temperature independent (strictly speaking, they do not include explicitly the temperature variable). The sum of them is the temperature-independent contribution to i level from EPI, which is similar to the Lamb shift due to the interaction of the atomic systems with the ''zero electromagnetic field.'' [27] In fact, it results from the interaction between the localized electronic state and the zero-point vibration of the lattice.

At a constant temperature, the contribution to i level from EPI changes with pressure, which causes the PS of i level due to EPI.

III. CALCULATIONS OF NORMAL-PRESSURE ENERGY SPECTRA AND g FACTORS

A. Normal-pressure energy spectra

As is well known, in GSGG:Cr^{3+}, the Cr^{3+} ion substitutes for the Sc^{3+} ion and enters a site with trigonally distorted octahedral symmetry. The open shell of the Cr^{3+} ion has a $(3d)^3$ electronic configuration. For convenience, the strong-field scheme and trigonal bases are adopted.[28] Similar to Refs. 12 and 16, with all the matrix elements of the cubic field (in terms of Dq), trigonal field ($\sim K$ and K'), Coulomb interaction between d electrons ($\sim B$ and C), and spin-orbit interaction ($\sim\zeta$ and ζ'), we have constructed the 120×120 complete energy matrix of d^3 electronic configuration in a trigonally distorted cubic field.

In order to determine the values of parameters at normal pressure, we adopt the observed results in Refs. 1–3 and 29–33 for low excited states $t_2^3\,{}^2E$, $t_2^2({}^3T_1)e\,{}^4T_2$, and $t_2^3\,{}^2T_1$ of GSGG:Cr^{3+} (see the latter text), since they are more accurate. In Ref. 33, the values of Dq_0, B_0, C_0, $V_0=-3K_0$, $V_0'=-\sqrt{2}K_0'$, ζ_0 were determined by fitting a lot of observed data of optical spectra of GSGG:Cr^{3+} (including the one for higher excited states), where the approximation $\zeta_0=\zeta_0'$ was made. According to Ref. 33, $\zeta_0(=\zeta_0')$ was 170 cm^{-1}, which is adopted for 70 and 300 K in this work, because its dependence on temperature is insignificant. However, according to this work, the values of Dq_0, B_0, C_0, K_0, and K_0' given by Ref. 33 should be changed (see the latter text). As was mentioned in Sec. II A, the approximation $K_0=K_0'$ can be made for GSGG:Cr^{3+}. Thus it is necessary to determine the values of only four parameters, Dq_0, B_0, C_0, and K_0.

By using aforementioned observed results[1–3,29–33] and by means of diagonalization of the complete d^3 energy matrix (DCEM), after taking into account the contributions to energy spectra from EPI (see the latter text), we have determined the values of the four parameters at 300 K and normal

pressure $Dq_0=1472\ \mathrm{cm}^{-1}$, $B_0=652.0\ \mathrm{cm}^{-1}$, $C_0=3251\ \mathrm{cm}^{-1}$, $K_0=-87\ \mathrm{cm}^{-1}$, and the whole energy spectrum and wave functions (without EPI) have also been obtained. Similarly, the values of the four parameters at 70 K and normal pressure have been determined: $Dq_0=1476\ \mathrm{cm}^{-1}$, $B_0=652.7\ \mathrm{cm}^{-1}$, $C_0=3253\ \mathrm{cm}^{-1}$, $K_0=-90\ \mathrm{cm}^{-1}$. The corresponding whole energy spectrum and wave functions (without EPI) have also been obtained.

The differences between the values of parameters at 300 K and those at 70 K are mainly the increases of Dq_0 and $|K_0|$ with decreasing temperature. Physically, this means the increase of crystal-field strength (corresponding to the decrease of interionic distance) with decreasing temperature. So, in view of the thermal expansion, this is reasonable. Because $\overline{E}[t_2^2(^3T_1)e\ ^4T_2]$ is almost equal to $10Dq_0$, while $\overline{E}[t_2^3\ ^2E]$ depends only slightly on Dq_0, the average energy separation $\Delta=\overline{E}[t_2^2(^3T_1)e\ ^4T_2]-\overline{E}[t_2^3\ ^2E]$ increases with decreasing temperature. In previous work, however, Δ was determined by neglecting the spin-orbit interaction H_{so} and trigonal field V_{trig} (i.e., $\zeta_0=K_0=0$). By using DCEM as well as the values of Dq_0, B_0, and C_0 at 300 K and $\zeta_0=K_0=0$, we get the value of Δ to be 187.5 cm^{-1} at 300 K and normal pressure; similarly, we get the value of Δ to be 215.7 cm^{-1} at 70 K and normal pressure. Therefore we have $\delta\Delta/\delta T\cong-0.12\ \mathrm{cm}^{-1}/\mathrm{K}$, which is close to the value $-0.15\ \mathrm{cm}^{-1}/\mathrm{K}$ given by Ref. 9.

In this work, we have found that it is essential to take into account H_{so} and V_{trig}. In Ref. 8, a similar conclusion was given. In GSGG:Cr^{3+}, there are four nonequivalent Cr^{3+} sites with different strengths of crystal fields, which causes the values of their Δ to be very different.[29–32] Besides, the energy separations between $t_2^2(^3T_1)e\ ^4T_2$ (including six levels) and $t_2^3\ ^2E$ (including two levels) are comparable to splittings of $t_2^2(^3T_1)e\ ^4T_2$ for GSGG:Cr^{3+}. Thus we can only speak of an effective or average energy separation between $t_2^2(^3T_1)e\ ^4T_2$ and $t_2^3\ ^2E$.[9,31,32]

Now, we calculate the contributions to energy spectra from EPI. The detailed calculations show that at a constant temperature, the ratio of the optical-branch term to the acoustic-branch term is almost unchanged with pressure; moreover, the contribution of the optical-branch term is obviously smaller than the one of the acoustic-branch term. Thus, for the calculation at a constant temperature and under various pressures, we may approximately take the sum of the acoustic-branch term and the optical-branch term as the acoustic-branch term multiplying a factor C_a ($C_a>1$, and it is approximately considered as a constant).

In calculation of $\langle\psi_i^{\mathrm{el}}|C(T_2M)|\psi_j^{\mathrm{el}}\rangle$, $\langle\psi_i^{\mathrm{el}}|C(EM)|\psi_j^{\mathrm{el}}\rangle$, and $\langle\psi_i^{\mathrm{el}}|D(T_2M)|\psi_i^{\mathrm{el}}\rangle$, all the reduced matrix elements of $C(T_2)$, $C(E)$, and $D(T_2)$ for three electrons are virtually expressed in terms of six reduced matrix elements for a single electron $Y_c(\equiv\langle t_2\|C(T_2)\|t_2\rangle)$, $Z_c(\equiv\langle t_2\|C(T_2)\|e\rangle)$, $P_c(\equiv\langle t_2\|C(E)\|t_2\rangle)$, $Q_c(\equiv\langle e\|C(E)\|e\rangle)$, $Y_d(\equiv\langle t_2\|D(T_2)\|t_2\rangle)$, and $Z_d(\equiv\langle t_2\|D(T_2)\|e\rangle)$. The values of Y_c, Z_c, P_c, Q_c, Y_d, and Z_d may be determined from the observed data of the stress-induced changes in splittings and the thermal shifts of optical spectra.[22] At the present time, however, there are no these observed data for GSGG:Cr^{3+}. Hence we have to take approximately the values of Y_c, Z_c, P_c, Q_c, Y_d, and Z_d of GSGG:Cr^{3+} as corresponding values of ruby (see Ref. 22) multiplying an adjustable factor C_b, which takes already into account the differences between properties (such as the strength of EPI, elastic properties and density) of GSGG:Cr^{3+} and ruby. So, in the calculation, the value of $(1/\rho)(1/\nu_l^5+3/2\,\nu_t^5)$ for ruby is also adopted.[22] By combining C_a and C_b, only an adjustable parameter $C_m=C_a\times C_b$ is necessary.

We fail to find the datum of T_D of GSGG:Cr^{3+}. According to Ref. 34, T_D of $Y_3Al_5O_{12}$(YAG):Cr^{3+} is 700–750 K, and T_D of ruby is 935–1030 K. These results were obtained by fitting the specific heat and by taking into account all phonon branches. However, according to Ref. 22, T_D of acoustic branches of ruby is 780 K. Therefore T_D of acoustic branches of YAG:Cr^{3+} should approximately be $(750/1030)\times780\ \mathrm{K}=568\ \mathrm{K}$. Because the distance between Cr^{3+} and ligand ions of GSGG:Cr^{3+} is larger than the one of YAG:Cr^{3+} and accordingly the crystal field and force constants of GSGG:Cr^{3+} are smaller than those of YAG:Cr^{3+}, T_D of acoustic branches of GSGG:Cr^{3+} should be smaller than T_D of acoustic branches of YAG:Cr^{3+}. As a reasonable approximation, we can take $T_D\sim500\ \mathrm{K}$ for acoustic branches of GSGG:Cr^{3+}.

By using the aforementioned results as well as the electronic wave functions and energy spectra obtained by DCEM, with fitting the observed results of optical spectra of GSGG:Cr^{3+} and their PS's,[1–3,29–33] we have determined $C_m=0.79$ (see the latter text). Namely, from this and Ref. 22, we have $Y_c=2.36\times10^4\ \mathrm{cm}^{-1}$, $Z_c=-5.19\times10^4\ \mathrm{cm}^{-1}$, $P_c=-2.08\times10^4\ \mathrm{cm}^{-1}$, $Q_c=2.65\times10^4\ \mathrm{cm}^{-1}$, $Y_d=2.55\times10^6\ \mathrm{cm}^{-1}$, and $Z_d=6.61\times10^5\ \mathrm{cm}^{-1}$ for GSGG:Cr^{3+}.

Then, by using Eqs. (24) and (26)–(29) as well as the wave functions and energy spectra obtained by DCEM, the contributions to various spectral lines (or bands) from EPI have been evaluated at 300 and 70 K. The calculation is carried out with the FORTRAN program worked out by us. We compare the total calculated results with the observed ones as follows.

(i). At 4.2 K and normal pressure, by taking the weight-mean of observed R_1 lines of four nonequivalent Cr^{3+} sites in GSGG:Cr^{3+} (with their intensity ratios as the weights),[29–30] the R_1-line transition energy is $\sim14\,370\ \mathrm{cm}^{-1}$ (it is in agreement with the observed value at 70 K in Refs. 1 and 2). Similarly, the weight mean of four observed R_1-R_2 separations is $\sim25.5\ \mathrm{cm}^{-1}$.[29] The total calculated result is the algebraic sum of pure electronic result (hereafter, it is the first term) and EPI result (hereafter, it is the second term). From above-mentioned calculations, we obtain the R_1-line transition energy to be $14405.6\ \mathrm{cm}^{-1}-35.4\ \mathrm{cm}^{-1}=14\,370.2\ \mathrm{cm}^{-1}$, which is in very good agreement with aforementioned observed value. Moreover, we obtain the calculated R_1-R_2 separation to be $21.3\ \mathrm{cm}^{-1}+4.7\ \mathrm{cm}^{-1}=26.0\ \mathrm{cm}^{-1}$, which is also in good agreement with its observed value.

At 300 K and normal pressure, by taking into account the R_1-line redshift from 70 to 300 K (it is approximately esti-

mated on the basis of the observed data in Ref. 3), the R_1-line transition energy of GSGG:Cr^{3+} should be ~14328 cm^{-1}, which is considered as an "experimental" value (noticing that no indication of R_1 line of GSGG:Cr^{3+} was seen at 300 K and normal pressure[2]). This is in very good agreement with the calculated result 14386.9 $cm^{-1}-59.2$ cm^{-1} $=14\,327.7$ cm^{-1}. Moreover, by making an extrapolation on the basis of observed R_1-R_2 separations at various high pressures,[2] the R_1-R_2 separation at 300 K and normal pressure is ~29 cm^{-1}. This is also in very good agreement with the calculated result 21.5 $cm^{-1}+7.6$ $cm^{-1}=29.1$ cm^{-1}. It is noteworthy that the observed results of R_1 and R_2 sharp lines are the most accurate in all optical spectral data, and accordingly they should principally considered in the fitting procedure.

(ii). At low temperature and normal pressure, according to Table III of Ref. 33, the observed peak position of the U absorption band was ~15 719 cm^{-1}, which is in good agreement with the calculated result 14781 $cm^{-1}-189$ cm^{-1} $+2290/2$ $cm^{-1}=15\,737$ cm^{-1}. Here, the algebraic sum of the first term and the second one is the zero-phonon energy of the U band (including the effect of EPI), and the third term is half of the Stokes shift (its value is taken from Ref. 3). As is well known, there is a large Stokes shift between the U absorption band and the U emission band, due to lattice vibration relaxation. Hence the transition energy of the U absorption band is equal to its zero-phonon energy plus half of the Stokes shift, and the transition energy of the U emission band is equal to its zero-phonon energy minus half of the Stokes shift (e.g., see Refs. 3, 31, 32, 35, and 36). It should be mentioned that there is no Stokes shift for R_1 and R_2 sharp lines.

At 300 K and normal pressure, the observed peak position of the U emission band was ~740 nm (~1.35 $\times 10^4$ cm^{-1}),[2] which is in good agreement with the calculated result 14 745 $cm^{-1}-191$ $cm^{-1}-2290/2$ cm^{-1} $=13\,409$ cm^{-1} within the observed error of the broad band. Moreover, the observed peak position of the U absorption band was ~15 625 cm^{-1},[3] which is in good agreement with the calculated result 14745 $cm^{-1}-191$ cm^{-1} $+2290/2$ $cm^{-1}=15\,699$ cm^{-1}.

(iii). At low temperature and normal pressure, two sharp lines were observed at 15 074 and 15 298 cm^{-1}.[33] According to the present work, they should be assigned to the R_3' line ($t_2^3\,{}^4A_2\rightarrow t_2^3\,{}^2T_1\pm 1/2a_0$ transition) and the R_1' line ($t_2^3\,{}^4A_2$ $\rightarrow t_2^3\,{}^2T_1\pm 1/2a_{\mp}$ transition), respectively. Their calculated results are 15 102 $cm^{-1}+29$ $cm^{-1}=15\,131$ cm^{-1} and 15 189 $cm^{-1}+27$ $cm^{-1}=15\,216$ cm^{-1}, respectively, which are in good agreement with the observed results within experimental error.

In a word, the values of normal-pressure parameters Dq_0, B_0, C_0, and K_0 at 70 and 300 K are obtained by fitting to observed results of R_1, R_2, R_3', and R_1' lines as well as absorption and emission U bands at low and room temperatures. By making a comparison between the values of these parameters at 70 and 300 K, only a small adjustment (mainly for Dq_0 and K_0) occurs. As was mentioned, the reasonableness of the adjustment is supported by the fact that the calculated result of $\delta\Delta/\delta T$ is in accord with the value given by Ref. 9. Further, as will be seen, the reasonableness of the values of these parameters is supported by the agreement between the calculated and experimental results of $g_{\parallel}(R_1)$ and $g_{\perp}(R_1)$ as well as PS's of the R_1 line, the R_2 line, and the U band at 300 and 70 K. As for the value of C_m, it is preliminarily determined by above-mentioned calculation, and its improvement will be carried out by the calculations fitting to PS's of the R_1 line, the R_2 line, and the U band at 300 and 70 K.

It should be mentioned that the value of Dq_0 was taken as 1450 cm^{-1} in Ref. 33. As is well known, the average energy of $t_2^2({}^3T_1)e\,{}^4T_2$ is almost $10Dq_0$. In Ref. 33, obviously, six observed lines from 14 420 to 14754 cm^{-1} were assigned to $t_2^2({}^3T_1)e\,{}^4T_2$ (see Table III of Ref. 33). The assignments and the value of Dq_0 are incorrect. In fact, according to observed absorption spectra at 4.2 K given by Table III of Ref. 33, the peak position of the strong absorption band with the lowest energy and largest bandwidth was at 15 719 cm^{-1}, which should be U absorption band [$t_2^3\,{}^4A_2\rightarrow t_2^2({}^3T_1)e\,{}^4T_2$ transition]. Moreover, this is demonstrated by the observed value 15 625 cm^{-1} of the U absorption band at 300 K,[3] because the redshift of the U absorption band from 4.2 to 300 K was -94 cm^{-1}, which is in agreement with Refs. 4, 31 and 37. The aforementioned six lines (they are just above R lines) may be assigned to the phonon satellite lines (i.e., phonon sidebands) of R lines, since many authors pointed out that there are R lines and their phonon sidebands in low-temperature optical spectra.[3,5–7,30,35] Thus, according to this work, we have obtained the important conclusion that traditional ligand-field theory should be improved by taking into account both the pure electronic contribution and the EPI one (including the Stokes shift for the U band). Only in this way can we obtain good agreement between calculated and observed results of R_1, R_2, R_3', and R_1' lines as well as absorption and emission U bands for GSGG:Cr^{3+}. Similarly, the normal-pressure optical spectra of ruby and their PS's have also been successfully calculated and explained, which will be reported elsewhere.

B. $g_{\parallel}(R_1)$ and $g_{\perp}(R_1)$

As is well known, due to the combined effect of the trigonal field and spin-orbit interaction, $t_2^3\,{}^2E$ is split into two Kramers doublets $t_2^3\,{}^2E\pm 1/2u_{\mp}$ [i.e., $t_2^3\,{}^2E(\bar{E})$] and $t_2^3\,{}^2E$ $\pm 1/2u_{\pm}$ [i.e., $t_2^3\,{}^2E(2\bar{A})$]. The transitions $t_2^3\,{}^2E(\bar{E})$ $\rightarrow t_2^3\,{}^4A_2$ and $t_2^3\,{}^2E(2\bar{A})\rightarrow t_2^3\,{}^4A_2$ correspond to the R_1 line and the R_2 line, respectively.

According to Ref. 38, the g values of R_1 ($t_2^3\,{}^2E$ $\pm 1/2u_{\mp}$) excited state can be calculated by using

$$g_{\parallel}=\frac{\left\langle t_2^3\,{}^2E-\frac{1}{2}u_+\right|'(L_z+g_sS_z)\left|t_2^3\,{}^2E-\frac{1}{2}u_+\right\rangle'}{\left\langle\frac{1}{2},\frac{1}{2}\right|S_z\left|\frac{1}{2},\frac{1}{2}\right\rangle}$$

$$=2\left\langle t_2^3\,{}^2E-\frac{1}{2}u_+\right|'(L_z+g_sS_z)\left|t_2^3\,{}^2E-\frac{1}{2}u_+\right\rangle', \tag{35}$$

$$g_{\perp}=\frac{\left|\left\langle t_2^3\,{}^2E\frac{1}{2}u_-\right|'(L_x+g_sS_x)\left|t_2^3\,{}^2E-\frac{1}{2}u_+\right\rangle'\right|}{\left\langle\frac{1}{2},\frac{-1}{2}\middle|S_x\middle|\frac{1}{2},\frac{1}{2}\right\rangle}$$
$$=2\left|\left\langle t_2^3\,{}^2E\frac{1}{2}u_-\right|'(L_x+g_sS_x)\left|t_2^3\,{}^2E-\frac{1}{2}u_+\right\rangle'\right|$$
$$=2\left|\left\langle t_2^3\,{}^2E\frac{1}{2}u_-\right|'\left(\frac{L_{-1}^{(1)}}{\sqrt{2}}+\frac{g_s}{2}S^-\right)\left|t_2^3\,{}^2E-\frac{1}{2}u_+\right\rangle'\right|, \tag{36}$$

where $g_s=2.0023$ is the free-spin (or spin-only) g value. It is more convenient to adopt the operators $S^-=S_x-iS_y$ and $L_{-1}^{(1)}=1/\sqrt{2}(L_x-iL_y)$. In Refs. 38 and 39, all the matrix elements of L_z and $L_{-1}^{(1)}$ were calculated. They are expressed in terms of the orbital-angular-momentum reduction factors k and k', and $k'=(1-\varepsilon)^{1/2}k$ for octahedral fields (ε is the covalency parameter). In Eqs. (35) and (36), the prime indicates that all the admixtures of base wave functions within d^3 electronic configuration have been taken into account.

In Ref. 40, it was pointed out that only the transition from the component $t_2^3\,{}^2E-1/2u_+$ was observed for $t_2^3\,{}^2E(\overline{E})$ at liquid-helium temperature. For the sake of simplification, the electronic wave functions of $t_2^3\,{}^2E-1/2u_+$ and $t_2^3\,{}^2E1/2u_-$ states obtained by DCEM without EPI are adopted; the values of k and ε are reasonably taken as the ones for ruby, i.e., $k=0.63$ and $\varepsilon=0.20$.[12,38] In this way, without fitting procedure, we have theoretically evaluated out $g_{\parallel}^{\rm calc}(R_1)=-2.62$ and $g_{\perp}^{\rm calc}(R_1)=0.03$ for the R_1 $[t_2^3\,{}^2E(\overline{E})]$ excited state of GSGG:Cr^{3+}, which are in good agreement with the experimental results $|g_{\parallel}^{\rm exp}(R_1)|=2.6\pm0.05$ and $g_{\perp}^{\rm exp}(R_1)<0.1$.[41] It is noteworthy that $g_{\parallel}^{\rm exp}(R_1)=-2.445\pm0.001$ and $g_{\perp}^{\rm exp}(R_1)=0.0515\pm0.0001$ for ruby,[38,42,43] which are close to the values of $g_{\parallel}^{\rm exp}(R_1)$ and $g_{\perp}^{\rm exp}(R_1)$ for GSGG:Cr^{3+}, respectively. The agreement between the calculated and experimental results of $g_{\parallel}(R_1)$ and $g_{\perp}(R_1)$ have once more demonstrated the reasonableness of the wave functions obtained by DCEM and the values of parameters resulting in these wave functions.

IV. CALCULATIONS OF PS's OF R_1 LINE, R_2 LINE, AND U BAND AT 300 AND 70 K

By using the values of parameters at normal pressure, B_0, C_0, Dq_0, K_0, K_0', ζ_0, and ζ_0', the P-χ dependence and the expressions of B, C, Dq, K, K', ζ, and ζ' as functions of χ, and using a least-square fit to the experimental data of PS's of the R_1 line, the R_2 line, and the U band for GSGG:Cr^{3+} at 300 K by making calculations of both pure electronic PS and EPI PS, the values of parameters for PS at 300 K have been determined as $S=0.699$, $D_1=-15.2$, $t=4.56$, and $A_1=A_2=-6.69\times10^3$ cm^{-1}. Similarly, by using a least-square fit to the experimental data of PS of its R_1 line at 70 K, we have determined $S=0.756$, $D_1=-15.8$, $t=1.54$, and $A_1=A_2=-7.01\times10^3$ cm^{-1} at 70 K. In fitting procedure, at 300 K, the observed data of PS's of the R_1 line and the R_2 line at many pressures and PS of the U band at low-pressure range are employed.[2] Thus the values of S, D_1, t, A_1, and the ratio factor in Eq. (16) can be determined. Moreover, the value of C_m has further been determined, with smaller uncertainty. At 70 K, there were the observed data of PS's of the R_1 line at many pressures.[1,2] It is found that only small adjustment between the values of S, D_1, t, and A_1 at 300 K and those at 70 K (mainly for t) is necessary. Thus this adjustment can readily be carried out. From 300 to 70 K, the decrease of t gives rise to the increases of Dq, $|K|$, and $|K'|$, which is consistent with the results in Sec. III. Besides, in calculations of PS's of the R_1 line, the R_2 line, and the U band at 300 and 70 K, the reasonableness of the value of T_D estimated in Sec. III has also been demonstrated.

Then, with the obtained values of parameters, from the P-χ dependence and expressions of Dq, B, C, ζ, ζ', K, and

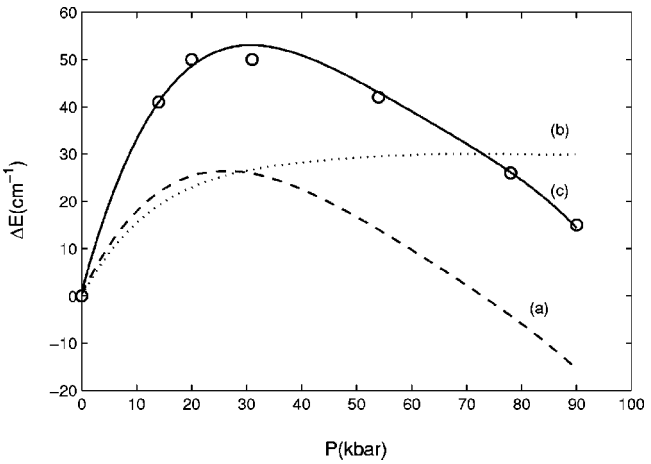

FIG. 1. The PS of the R_1 line of GSGG:Cr^{3+} at 70 K. Curve (a) is the PS of the R_1 line without EPI (the pure electronic PS) $\Delta E^{\rm el}$; curve (b) is the PS of the R_1 line due to EPI ΔE^{e-p}; curve (c) is the total PS of the R_1 line $\Delta E_{\rm total}^{\rm calc}$. The experimental points (○) are taken from Ref. 2.

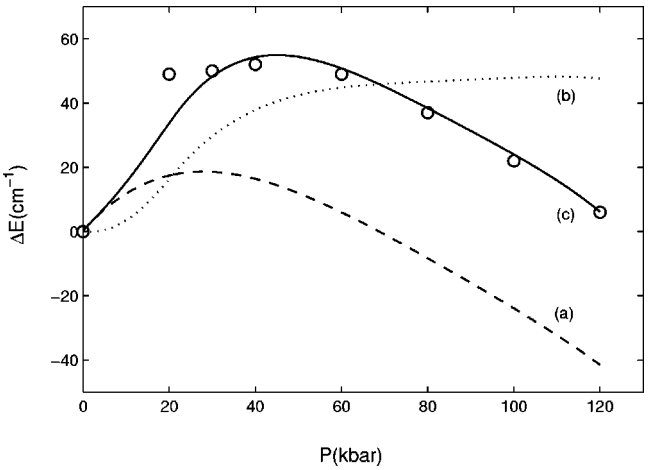

FIG. 2. The PS of the R_1 line of GSGG:Cr^{3+} at 300 K. Curve (a) is the PS of the R_1 line without EPI (the pure electronic PS) $\Delta E^{\rm el}$; curve (b) is the PS of the R_1 line due to EPI ΔE^{e-p}; curve (c) is the total PS of the R_1 line $\Delta E_{\rm total}^{\rm calc}$. The experimental points (○) are taken from Ref. 2.

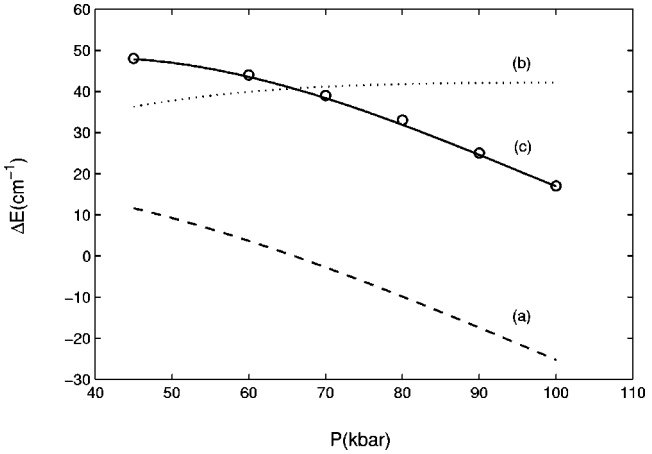

FIG. 3. The PS of the R_2 line of GSGG:Cr^{3+} at 300 K. Curve (a) is the PS of the R_2 line without EPI (the pure electronic PS) ΔE^{el}; curve (b) is the PS of the R_2 line due to EPI ΔE^{e-p}; curve (c) is the total PS of the R_2 line $\Delta E^{\mathrm{calc}}_{\mathrm{total}}$. The experimental points (○) are taken from Ref. 2.

K' as functions of χ, the energy spectra and wave functions of GSGG:Cr^{3+} at various pressures and temperatures can be finally obtained by DCEM. Therefore PS's of energy spectra without EPI at 300 and 70 K have been evaluated respectively. They are pure electronic PS ΔE^{el}. The calculation is carried out with the FORTRAN program worked out by us. The calculated results of ΔE^{el} of the R_1 line for GSGG:Cr^{3+} at 70 K are shown in Fig. 1. For PS's of the R_2 line and the U band for GSGG:Cr^{3+}, there are only the experimental data at 300 K.[2] The calculated results of ΔE^{el} of the R_1 line and the R_2 line at 300 K are shown in Figs. 2 and 3, respectively. The calculated results of ΔE^{el} of the R_1 line at 300 K are also listed in Table II. At 300 K, the average rates of pure electronic PS of the U band in various ranges of pressure are listed in Table I. The average PS of the U band is the average of PS's of six levels for $t_2^2(^3T_1)e^4T_2$.

Similarly to the calculation in Sec. III A, at 300 or 70 K, the contributions to the R_1 line, the R_2 line, and the U band from EPI under various pressures and accordingly their PS's have been calculated. In the calculation, the contribution to the R_1 line is the one to R_1 level minus the one to the ground level, and so on. The PS of the R_1 line (or the R_2 line or the U band) due to EPI consists of the temperature-independent part ΔE_0^{e-p} and temperature-dependent one ΔE_T^{e-p}. Namely, we have

$$\Delta E^{e-p}=\Delta E_0^{e-p}+\Delta E_T^{e-p}. \tag{37}$$

By taking into account both the PS of the R_1 line (or the R_2 line or the U band) due to EPI and the pure electronic PS, we get the total calculated result of PS of the R_1 line (or the R_2 line or the U band),

$$\Delta E^{\mathrm{calc}}_{\mathrm{total}}=\Delta E^{\mathrm{el}}+\Delta E^{e-p}. \tag{38}$$

The calculated results of ΔE^{e-p} and $\Delta E^{\mathrm{calc}}_{\mathrm{total}}$ of the R_1 line for GSGG:Cr^{3+} at 70 K are shown in Fig. 1, together with the experimental points.[1,2] Similarly, the calculated and experimental results of the R_1 line and the R_2 line at 300 K are shown in Figs. 2 and 3, respectively. The average rate of PS of the U band due to EPI, its pure electronic average rate of PS, and its total average rate of PS are listed in Table I. In 0–20 kbar, the total average rate of PS of the U band is 11.25 cm^{-1}/kbar, which is in good agreement with its observed value 10 ± 2 cm^{-1}/kbar in the range of low pressure (<25 kbar).[2] Moreover, the calculated results of ΔE^{e-p} and $\Delta E^{\mathrm{calc}}_{\mathrm{total}}$ of the R_1 line at 300 K as well as various contributions to them are also listed in Table II.

It is shown that the calculated results are in good agreement with all the experimental data within experimental errors.[2] Nevertheless, we should note the remarkable departure of the calculated result of the R_1 line PS at 20 kbar and

TABLE I. Average rates of pressure-induced shifts of the U band for GSGG:Cr^{3+} at 300 K and various pressure ranges.[a]

Pressure range (kbar)	Pure electronic contribution (cm^{-1}/kbar)	Contribution from EPI (cm^{-1}/kbar)	Total average rate of PS (cm^{-1}/kbar)
0–20	8.67	2.58	11.25
20–40	11.46	1.46	12.92
40–80	8.39	0.39	8.78
80–120	9.14	2.41	11.55

[a]At 300 K, the observed value of the total average rate of PS of the U band in the range of low pressure (<25 kbar) was 10 (±2) cm^{-1}/kbar (Ref. 2).

TABLE II. P-χ dependence and pressure-induced shifts (relative to normal pressure) of the R_1 line of GSGG:Cr^{3+} at 300 K and various contributions to them, in unit cm^{-1}.

P (kbar)	χ	ΔE_0^{e-p}	ΔE_T^{e-p}	ΔE^{e-p}	ΔE^{el}	$\Delta E^{\mathrm{calc}}_{\mathrm{total}}$	$\Delta E^{\mathrm{exp\ a}}_{\mathrm{total}}$
20	0.997 300	20.91	−4.76	16.15	17.46	33.61	49
30	0.995 966	25.64	4.28	29.92	18.33	48.25	50
40	0.994 643	28.49	9.27	37.76	16.14	53.90	52
60	0.992 026	31.28	13.31	44.59	6.14	50.73	49
80	0.989 448	32.30	14.68	46.98	−7.99	38.99	37
100	0.986 908	32.59	15.12	47.71	−24.19	23.52	22
120	0.984 404	32.53	15.17	47.70	−41.41	6.29	6

[a]The data are taken from Fig. 4(b) in Ref. 2.

TABLE III. $\Delta_{R_1-{}^4T_2}$, $\delta(\Delta_{R_1-{}^4T_2})/\delta P$, ζ and admixtures of $|t_2^3\,{}^2E\pm\frac{1}{2}u_{\mp}\rangle$ and $|t_2^2({}^3T_1)e^4T_2\rangle$ in wave functions of the R_1 ($t_2^3\,{}^2E\pm\frac{1}{2}u_{\mp}$) level at 300 K and various pressures (without EPI).

P (kbar)	Sum of square mixing coefficients of $\|t_2^2({}^3T_1)e^4T_2\rangle$	Sum of square mixing coefficients of $\|t_2^3\,{}^2E\pm\frac{1}{2}u_{\mp}\rangle$	Their ratio	$\Delta_{R_1-{}^4T_2}$ (cm^{-1})	$\frac{\delta(\Delta_{R_1-{}^4T_2})}{\delta P}$ (cm^{-1}/kbar)	ζ (cm^{-1})
1 bar	0.292 21	0.681 72	0.428 64	358.21		170.00
15 kbar	0.180 26	0.789 48	0.228 33	456.66	6.56	169.86
30 kbar	0.115 49	0.851 28	0.135 67	615.65	10.60	169.72
40 kbar	0.088 477	0.876 68	0.100 92	744.75	12.91	169.64
60 kbar	0.055 645	0.906 62	0.061 376	914.66	8.50	169.48
80 kbar	0.037 764	0.921 63	0.040 975	1104.62	9.50	169.33
100 kbar	0.027 158	0.929 12	0.029 230	1302.26	9.88	169.20
120 kbar	0.020 414	0.932 39	0.021 894	1503.52	10.06	169.07

300 K from the observed one (see Table II and Fig. 2). In view of a large experimental error at 20 kbar and 300 K, further work is necessary.

V. PHYSICAL ORIGINS OF PS OF R_1 LINE, R_2 LINE, AND U BAND

For the sake of simplicity, only the physical origins of the PS of the R_1 line at 300 K and its reversal are investigated in detail.

A. Pure electronic contribution to PS of R_1 line

In generally, a wave function obtained by diagonalizing the 120×120 d^3 energy matrix of GSGG:Cr^{3+} is a linear combination of 120 trigonal base wave functions, and it (or corresponding level) is labeled by the symbol of the basis with the largest mixing coefficient. At 300 K, the mixing degrees of $|t_2^2({}^3T_1)e^4T_2\rangle$ and $|t_2^3\,{}^2E\pm1/2u_{\mp}\rangle$ base wave functions in the wave functions of R_1 ($t_2^3\,{}^2E\pm1/2u_{\mp}$) level (represented by the ratios in Table III) have been evaluated under various pressures. From Table III, at normal pressure, the degree of their admixture is remarkable, which quantitatively indicates that the R_1 ($t_2^3\,{}^2E\pm1/2u_{\mp}$) state has characteristics of both $t_2^3\,{}^2E\pm1/2u_{\mp}$ and $t_2^2({}^3T_1)e^4T_2$. The mixing degree rapidly decreases with increasing pressure. At 70 K, similar results have been also obtained. It is found that under the same pressure, the mixing degree of $|t_2^2({}^3T_1)e^4T_2\rangle$ and $|t_2^3\,{}^2E\pm1/2u_{\mp}\rangle$ in the wave functions of R_1 level at 300 K is always larger than the one at 70 K. This is mainly because the separation between R_1 level and the average of $t_2^2({}^3T_1)e^4T_2$ levels $\Delta_{R_1-{}^4T_2}$ at 300 K is always smaller than the one at 70 K (see Sec. III A).

Here, for the sake of simplification and convenience, the $|t_2^2({}^3T_1)e^4T_2\rangle$ base wave functions mix into the wave functions of R_1 level through the spin-orbital interaction, and EPI has not been considered. With increasing pressure, the increase of Dq [making $t_2^2({}^3T_1)e^4T_2$ levels rise] and the decrease of B and C (making the R_1 level descend) give rise to the increase of the separation between the R_1 level and the average of $t_2^2({}^3T_1)e^4T_2$ levels. At 300 K, it is found that in the range of about 15–45 kbar, first $t_2^2({}^3T_1)e^4T_2$ levels rapidly rise with pressure and accordingly merge with $t_2^3\,{}^2T_1$ levels, then the order of them reverses. The mergence and/or order reversion between $t_2^2({}^3T_1)e^4T_2$ and $t_2^3\,{}^2T_1$ levels cause the extra increases of $\Delta_{R_1-{}^4T_2}$ and $\delta(\Delta_{R_1-{}^4T_2})/\delta P$ over the aforementioned pressure range (see Table I). Moreover, ζ $(=\zeta')$ decreases with increasing pressure. Both the increase of $\Delta_{R_1-{}^4T_2}$ and the decrease of ζ $(=\zeta')$ give rise to the rapid decrease of the mixing degree of $|t_2^2({}^3T_1)e^4T_2\rangle$ and $|t_2^3\,{}^2E\pm1/2u_{\mp}\rangle$ in the wave functions of the R_1 level with increasing pressure.

Now, without EPI, we investigate the dependences of various levels and their PS's on various parameters representing microscopic interactions. By means of DCEM, the contributions from various parameters to the energy values of two levels [$t_2^3\,{}^2E\pm1/2u_{\mp}$ and $t_2^2({}^3T_1)e^4T_2\pm1/2x_{\pm}$] have been calculated at two pressures. From Table IV, it is clearly shown that at 120 kbar, $t_2^2({}^3T_1)e^4T_2$ depends principally on Dq and $t_2^3\,{}^2E\pm1/2u_{\mp}$ depends mainly on B and C; however, at normal pressure, the dependence of $t_2^3\,{}^2E\pm1/2u_{\mp}$ on Dq is also remarkable. The latter is exactly caused by the remarkable admixture of $|t_2^2({}^3T_1)e^4T_2\rangle$ and $|t_2^3\,{}^2E\pm1/2u_{\mp}\rangle$, which is characteristic of GSGG:Cr^{3+}. Further, at two pressures, the rates of PS's of the two levels without EPI and the contributions to them from various parameters are quantitatively calculated by DCEM. From Table V, we can see that the R_1 ($t_2^3\,{}^2E\pm1/2u_{\mp}$) level has the rate of blue PS (1.623 cm^{-1}/kbar) at 1 bar, which is also characteristic of GSGG:Cr^{3+}; however, at 120 kbar, it has the rate of red PS (-0.876 cm^{-1}/kbar), which is close to the rate of red PS of pure $|t_2^3\,{}^2E\pm1/2u_{\mp}\rangle$. This is mainly because the mixing degree of $|t_2^2({}^3T_1)e^4T_2\rangle$ and $|t_2^3\,{}^2E\pm1/2u_{\mp}\rangle$ in the wave functions of the R_1 level is remarkable and accordingly the contributions of Dq to the rate of PS of the R_1 level [through the factor $\partial E/\partial(Dq)\cdot\Delta(Dq)/\Delta P$ in Table V] is large at 1 bar; however, at 120 kbar, this mixing degree is small and accordingly $\partial E/\partial(Dq)\cdot\Delta(Dq)/\Delta P$ of the R_1 level is also small.

TABLE IV. Contributions from various parameters to two levels at 1 bar and 120 kbar (without EPI).

P	Level	$\partial E/\partial(Dq)\times Dq$	$\partial E/\partial B\times B$	$\partial E/\partial C\times C$	$\partial E/\partial\zeta\times\zeta$	$\partial E/\partial\zeta'\times\zeta'$	$\partial E/\partial K\times K$	$\partial E/\partial K'\times K'$	Sum
1 bar	$t_2^3\,{}^2E\pm\frac{1}{2}u_\mp$	4655.54	2921.07	7024.40	−10.03	−171.73	−27.44	−4.86	14 386.94
	$t_2^2({}^3T_1)e^4T_2\pm\frac{1}{2}x_\pm$	13 586.24	347.50	782.62	−15.10	5.72	−8.54	1.86	14 700.29
120 kbar	$t_2^3\,{}^2E\pm\frac{1}{2}u_\mp$	823.19	4065.30	9649.53	−16.02	−50.93	−95.26	−30.28	14 345.53
	$t_2^2({}^3T_1)e^4T_2\pm\frac{1}{2}x_\pm$	15 606.12	82.09	149.43	−0.25	33.06	−121.08	2.77	15 752.14

As for $t_2^2({}^3T_1)e^4T_2\pm 1/2x_\pm$ [it is a level in six levels of $t_2^2({}^3T_1)e^4T_2$], it always has a large rate of blue PS and results mainly from Dq.

The pure electronic rate of PS of the R_1 line is exactly the slope of the curve (a) in Fig. 2 (or Fig. 1). From the above argument, the following behavior can be derived. At 1 bar, the slope is positive. With increasing pressure, the mixing degree of $|t_2^2({}^3T_1)e^4T_2\rangle$ (it contributes a positive rate of PS) and $|t_2^3\,{}^2E\pm 1/2u_\mp\rangle$ (it contributes a negative rate of PS) in the wave functions of the R_1 level and accordingly the relative contribution of $|t_2^2({}^3T_1)e^4T_2\rangle$ decreases. As a result, the slope first decreases gradually and approaches zero. Then, it becomes negative, moreover, its absolute value increases gradually and approaches to the one of the pure $|t_2^3\,{}^2E\pm 1/2u_\mp\rangle$ at very high pressure. This is exactly the behavior of curve (a). It is noteworthy that there is a reversal of $\Delta E^{\rm el}$ with pressure.

Obviously, the behavior of curve (a) results mainly from the decrease of the mixing degree of $|t_2^2({}^3T_1)e^4T_2\rangle$ and $|t_2^3\,{}^2E\pm 1/2u_\mp\rangle$ in the wave functions of the R_1 level with pressure. Therefore it can be said that the variations of various microscopic interactions (they are represented in terms of Dq, B, C, K, K', ζ, and ζ') with pressure lead to the variation of the mixing degree of $|t_2^2({}^3T_1)e^4T_2\rangle$ and $|t_2^3\,{}^2E\pm 1/2u_\mp\rangle$ in the wave functions of the R_1 level, which plays a key role for the pure electronic PS of the R_1 line.

B. Contribution to PS of R_1 line from EPI

In order to reveal physical origins of PS of the R_1 line due to EPI, we have calculated various contributions to the R_1 line from EPI at various pressures (see Table VI). Among them, the off-diagonal contributions to the R_1 level from EPI include EPI of the R_1 level with all the levels other than the R_1 level, which consists of contributions from the second column to the fifth column in Table VI. The off-diagonal contributions to the ground level from EPI have similar meaning. The diagonal contribution to the R_1 level (or ground level) from EPI is the sum of the terms depending on F_{ii} for the R_1 level (or ground level), see Eqs. (28) and (29). The total contribution from EPI to the R_1 level minus the one to the ground level gives rise to the EPI contribution to the R_1 line. From Table VI, it can be seen that the terms changing remarkably with pressure are only the contribution of EPI of the R_1 level with $t_2^2({}^3T_1)e^4T_2$ levels and the contribution of EPI of the R_1 level with the R_2 ($t_2^3\,{}^2E\pm 1/2u_\pm$) level. Namely, they make a dominant contribution to the PS of the R_1 line due to EPI. Their changes with pressure come from the factor $F_1\equiv\sum_M|\langle\psi_i^{\rm el}|C(T_2M)|\psi_j^{\rm el}\rangle|^2+8\sum_M|\langle\psi_i^{\rm el}|C(EM)|\psi_j^{\rm el}\rangle|^2$ and the factor

$$F_2\equiv T_{ij}T^2\cdot\mathbf{P}\int_0^{T_D/T}\frac{x^3}{(e^x-1)[x^2-(T_{ij}/T)^2]}dx+\frac{1}{2}\mathbf{P}\int_0^{T_D}\frac{y^3}{y-T_{ij}}dy.$$

In the final analysis, the change of F_1 results mainly from the changes of the admixtures of $|t_2^2({}^3T_1)e^4T_2\rangle$ and $|t_2^3\,{}^2E\rangle$ in wave functions of the R_1, R_2, and $t_2^2({}^3T_1)e^4T_2$ levels with pressure, and the change of F_2 results from the change of energy gap ($E_i-E_j=k_BT_{ij}$) with pressure. Furthermore,

TABLE V. Contributions from various parameters to rates of pressure-induced shifts (without EPI) of two levels at 1 bar and 120 kbar (in unit $\rm cm^{-1}$/kbar).

P	Level	$\partial E/\partial(Dq)\cdot\Delta(Dq)/\Delta P$	$\partial E/\partial B\cdot\Delta B/\Delta P$	$\partial E/\partial C\cdot\Delta C/\Delta P$	$\partial E/\partial\zeta\cdot\Delta\zeta/\Delta P$	$\partial E/\partial\zeta'\cdot\Delta\zeta'/\Delta P$	$\partial E/\partial K\cdot\Delta K/\Delta P$	$\partial E/\partial K'\cdot\Delta K'/\Delta P$	Rate of PS
1 bar	$t_2^3\,{}^2E\pm\frac{1}{2}u_\mp$	2.919	−0.278	−0.668	0.001	0.009	−0.306	−0.054	1.623
	$t_2^2({}^3T_1)e^4T_2\pm\frac{1}{2}x_\pm$	8.519	−0.033	−0.075	0.001	∼0	−0.095	0.020	8.337
120 kbar	$t_2^3\,{}^2E\pm\frac{1}{2}u_\mp$	0.490	−0.239	−0.567	0.001	0.002	−0.428	−0.135	−0.876
	$t_2^2({}^3T_1)e^4T_2\pm\frac{1}{2}x_\pm$	9.299	−0.005	−0.009	∼0	0.001	−0.544	0.012	8.754

TABLE VI. Various contributions to R_1 line from EPI at various pressures (in unit cm^{-1}).

P	EPI of R_1 level with $t_2^2(^3T_1)e^4T_2$ levels	EPI of R_1 level with R_2 level	EPI of R_1 level with $t_2^3\,{}^2T_1$ levels	EPI of R_1 level with all the other levels	Diagonal EPI of R_1 level	Off-diagonal EPI of ground level	Diagonal EPI of ground level	EPI contribution to R_1 line E^{e-p}
1 bar	−45.71	−6.28	−1.74	−3.66	−4.76	−2.80	−0.14	−59.21
20 kbar	−29.59	−1.69	−6.59	−3.34	−4.80	−2.78	−0.17	−43.06
40 kbar	−8.29	−0.51	−7.22	−3.19	−5.19	−2.76	−0.19	−21.45
60 kbar	−6.68	−0.20	−1.84	−3.12	−5.73	−2.73	−0.22	−14.62
80 kbar	−3.77	−0.11	−1.89	−3.08	−6.34	−2.71	−0.25	−12.23
100 kbar	−2.33	−0.10	−2.00	−3.06	−6.98	−2.70	−0.27	−11.50
120 kbar	−1.53	−0.12	−2.15	−3.04	−7.63	−2.67	−0.29	−11.51

from detailed calculations, it is found that the change of the contribution of EPI of the R_1 level with $t_2^2(^3T_1)e^4T_2$ levels results mainly from F_1, although F_2 also has considerable effect; the change of the contribution of EPI of the R_1 level with the R_2 level results almost from F_1. Thus we can conclude that the changes of the admixtures of $|t_2^2(^3T_1)e^4T_2\rangle$ and $|t_2^3\,{}^2E\rangle$ in wave functions of R_1, R_2, and $t_2^2(^3T_1)e^4T_2$ levels with pressure play a key role for the PS of the R_1 line due to EPI.

Besides, from the fourth column (in the column we list the term, which is the contribution of EPI of the R_1 level with $t_2^3\,{}^2T_1$ levels) in Table VI, in contrast to the small variation of the absolute value of the term in range of 60–120 kbar, the absolute value of the term increases obviously when pressure changes from 1 bar to 20 kbar (or 40 kbar). This comes mainly from the mergence and/or order reversion between $t_2^2(^3T_1)e^4T_2$ and $t_2^3\,{}^2T_1$ levels in the range of about 15–45 kbar.

From the last column in Table VI, it is found that the contribution to the R_1 line from EPI E^{e-p} is always negative, its absolute value decreases monotonously with pressure, and it is almost unchanged at very high pressure. This is mainly caused by the monotonous decreases of mixing degrees of $|t_2^2(^3T_1)e^4T_2\rangle$ and $|t_2^3\,{}^2E\rangle$ in wave functions of R_1, R_2, and $t_2^2(^3T_1)e^4T_2$ levels with pressure. The contribution to the R_1 line from EPI at P minus the one at normal pressure gives rise to its PS relative to normal pressure, i.e., ΔE^{e-p} in Table II. The ΔE^{e-p} is always positive, and it increases monotonously with pressure. At very high pressure, it approaches saturation.

We can see that the behavior of curve (a) is quite different from the one of curve (b). It is the combined effect of them that causes the behavior of $\Delta E_{\text{total}}^{\text{calc}}$ [curve (c)]. Namely, there is a reversal in curve (a), curve (b) ascends monotonously and approaches saturation, and accordingly there is a reversal of the PS of the R_1 line $\Delta E_{\text{total}}^{\text{calc}}$ with pressure in curve (c). According to aforementioned arguments, the change of the mixing degree of $|t_2^2(^3T_1)e^4T_2\rangle$ and $|t_2^3\,{}^2E \pm 1/2u_{\mp}\rangle$ in the wave functions of the R_1 level with pressure plays a key role for the behavior of curve (a), and the changes of the admixtures of $|t_2^2(^3T_1)e^4T_2\rangle$ and $|t_2^3\,{}^2E\rangle$ in wave functions of R_1, R_2, and $t_2^2(^3T_1)e^4T_2$ levels with pressure play a key role for the behavior of curve (b).

C. PS of *U* band at 300 K

For the PS's of the R_2 line at 300 K and the R_1 line at 70 K, its physical origins may be discussed similarly to the PS of the R_1 line at 300 K.

Now, only the PS of the U band at 300 K is briefly discussed. First, the average rate of blue PS of the U band without EPI (i.e., pure electronic contribution) is remarkably larger than the one due to EPI (see Table I); moreover, it is also remarkably larger than the rate of blue PS of the R_1 line at 1 bar (see Table V). This is because the U band depends mainly on Dq and accordingly it has an obviously large value of $\partial E/\partial(Dq)\cdot\Delta(Dq)/\Delta P$. Second, the average rate of PS of the U band due to EPI in two ranges (20–40 kbar and 40–80 kbar) are especially small, in comparison with the other pressure ranges in Table I. This is mainly caused by the mergence and/or order reversion between $t_2^2(^3T_1)e^4T_2$ and $t_2^3\,{}^2T_1$ levels over the range of about 15–45 kbar. In order to justify the theoretically predicted fluctuation of the rate of PS of the U band with pressure, further experimental work is necessary.

VI. DISCUSSION AND CONCLUSIONS

In this work, by means of the theory for PS's of energy spectra, at 300 and 70 K, the energy spectra of GSGG:Cr^{3+} without EPI and their PS's have been calculated, respectively. Further, by means of the theory for shifts of energy spectra due to EPI, the contributions to the R_1 line, the R_2 line, the U band from EPI, and their PS's have been also calculated respectively by using the electronic wave functions and energy spectra obtained at various pressures and temperatures. The whole energy spectrum without EPI is obtained by diagonalizing the complete d^3 energy matrix in a trigonally distorted cubic field. In the calculations of the contributions due to EPI, the temperature-independent and temperature-dependent terms, all levels, all admixtures of electronic wave functions, all phonon branches, all irreduc-

ible representations, and their components have been taken into account. The total calculated results of the R_1 line, the R_2 line, the U band, and their PS's at 300 and 70 K are in good agreement with all the experimental data within the experimental errors. The calculated results of the R_3' line, the R_1' line, $g_{\|}(R_1)$, and $g_{\perp}(R_1)$ are also in good agreement with experiment. The physical origins of two parts of PS's have been explained. At normal pressure, it has also been found that traditional ligand-field theory should be improved by taking into account both the pure electronic contribution and the EPI one (including the Stokes shift).

From this work, we have obtained the following conclusions.

(i) Under normal pressure, for GSGG:Cr^{3+} at 300 K (or 70 K), the mixing degree of $|t_2^2(^3T_1)e^4T_2\rangle$ and $|t_2^3\,{}^2E \pm 1/2u_{\mp}\rangle$ bases in the wave functions of the R_1 level is remarkable. With increasing pressure, both the increase of $\Delta_{R_1-{}^4T_2}$ and the decrease of ζ $(=\zeta')$ give rise to the rapid decrease of the mixing degree of $|t_2^2(^3T_1)e^4T_2\rangle$ and $|t_2^3\,{}^2E \pm 1/2u_{\mp}\rangle$. Under the same pressure, the mixing degree of $|t_2^2(^3T_1)e^4T_2\rangle$ and $|t_2^3\,{}^2E \pm 1/2u_{\mp}\rangle$ bases in the wave functions of the R_1 level at 300 K is always larger than the one at 70 K.

(ii) At 300 K, in the contribution from EPI to the R_1 line (or the R_2 line or the U band) and its PS, both the temperature-independent part and the temperature-dependent one are important. However, at 70 K, the temperature-independent part is much larger than the temperature-dependent one. The former results from the interaction between the zero-point vibration of the lattice and the localized electronic state.

(iii) The change of the mixing degree of $|t_2^2(^3T_1)e^4T_2\rangle$ and $|t_2^3\,{}^2E \pm 1/2u_{\mp}\rangle$ bases in the wave functions of the R_1 level with pressure plays a key role for the pure electronic PS of the R_1 line (or the R_2 line) due to the interactions represented by Dq, B, C, ζ, ζ', K, and K', and the changes of the admixtures of $|t_2^2(^3T_1)e^4T_2\rangle$ and $|t_2^3\,{}^2E\rangle$ bases in wave functions of R_1, R_2, and $t_2^2(^3T_1)e^4T_2$ levels with pressure play a key role for the PS of the R_1 line (or the R_2 line) due to EPI.

(iv) The pressure-dependent behavior of ΔE^{el} is quite different from the one of ΔE^{e-p}. It is the combined effect of them that causes the behavior of the total PS of the R_1 line $\Delta E_{\mathrm{total}}^{\mathrm{calc}}$ with pressure, and a reversal of PS of the R_1 line with pressure has been explained.

(v) At 300 K, it is found that in the range of about 15–45 kbar, first $t_2^2(^3T_1)e^4T_2$ levels merge with $t_2^3\,{}^2T_1$ levels, then the order of them reverses, which may cause the fluctuation of the rate of PS for $t_2^2(^3T_1)e^4T_2$ (or $t_2^3\,{}^2T_1$) with pressure. There is a similar effect at 70 K.

With increasing pressure, the rapid change of $|t_2^2(^3T_1)e^4T_2\rangle$ base wave functions mixing into $t_2^3\,{}^2E$ states and the dramatic change of emission spectra for GSGG:Cr^{3+} take place. It is very important for controlling the tunable laser.

According to the orbital physics, an electron bound to or nearly localized on the specific ionic site has three attributes: charge, spin, and orbital. The d electrons of dopant transition-metal ions in an ionic crystal possess nearly localized states, and the d orbital represents the shape of the d-electron wave function. The orbital physics will be a key concept for the science and technology of correlated electrons.[44] From the viewpoint of the orbital physics and ligand-field theory, the crystal field represents the Coulomb interaction of the d orbital of the central transition-metal ion with the other ions of the crystal and the core of the central ion; $10Dq$ represents the splitting due to cubic crystal field, which is the energy difference between e_g orbitals and t_{2g} orbitals in octahedral crystal field; B and C represent the Coulomb interaction between d orbitals; ζ and ζ' represent the spin-orbit interaction of the d electron. From this work thus d orbitals and interactions relevant to them are very important.

For ruby, MgO:Cr^{3+} and MgO:V^{2+}, there were observed data of the thermal shifts of R lines and the U band as well as the isotope shifts of R lines, and accordingly effects of EPI can solely be observed (e.g., see Refs. 20–25). Unfortunately, at present, there were no observed data for GSGG:Cr^{3+}. The pure electronic contribution and the EPI one to optical spectra or their PS's cannot be solely observed. However, the two contributions to various spectral lines (or bands) may have the same or opposite signs (see Sec. III A). Especially the two contributions to PS's of R_1 and R_2 lines have quite different behaviors (see Sec. V). In the lower pressure range, they strengthen each other, but in the higher pressure range, they cancel each other. At very high pressures, ΔE^{e-p} approaches saturation, and accordingly the variation of PS (i.e., the rate of PS) results from almost only pure electronic contribution. Hence, by fitting to a lot of aforementioned observed data (including approximately smooth experimental curves of PS's of R_1 and R_2 lines), the uncertainties of the obtained values of parameters and the division between the pure electronic part and the EPI one are small. It can be said that the theory and results of the present work are reasonable.

*Corresponding address. Email address: maurice@mail.sc.cninfo.net

[1] U. Hommerich and K. L. Bray, Phys. Rev. B **51**, 8595 (1995).
[2] U. Hommerich and K. L. Bray, Phys. Rev. B **51**, 12 133 (1995).
[3] B. Struve and G. Huber, Appl. Phys. B: Photophys. Laser Chem. **36**, 195 (1985).
[4] C. J. Donnelly, S. M. Healy, T. J. Glynn, G. F. Imbusch, and G. P. Morgan, J. Lumin. **42**, 119 (1988).
[5] C. J. Donnelly, T. J. Glynn, G. P. Morgan, and G. F. Imbusch, J. Lumin. **48&49**, 283 (1991).
[6] M. Yamaga, B. Henderson, and K. P. O'Donnell, J. Phys.: Condens. Matter **1**, 9175 (1989).
[7] M. Yamaga, B. Henderson, and K. P. O'Donnell, Phys. Rev. B **46**, 3273 (1992).
[8] A. J. Wojtowicz, M. Grinberg, and A. Lempicki, J. Lumin. **50**, 231 (1991).

[9] M. Grinberg, J. Lumin. **54**, 369 (1993).
[10] X. Wu, S. Huang, U. Hommerich, W. M. Yen, B. G. Aitken, and M. Newhouse, Chem. Phys. Lett. **233**, 28 (1995).
[11] Ma Dong-ping, Ma Ning, Lin Qang, and Chen Ju-rong, Commun. Theor. Phys. **34**, 605 (2000).
[12] Ma Dong-ping, Zhang Hong-mei, Liu Yan-yun, Chen Ju-rong, and Ma Ning, J. Phys. Chem. Solids **60**, 463 (1999).
[13] Ma Dong-ping, Ma Xiao-dong, Chen Ju-rong, and Liu Yan-yun, Phys. Rev. B **56**, 1780 (1997).
[14] Ma Dong-ping, Ma Ning, Ma Xiao-dong, and Zhang Hong-mei, J. Phys. Chem. Solids **59**, 1211 (1998).
[15] Ma Dong-ping, Wang Zao-qing, Chen Ju-rong, and Zhang Zheng-gang, J. Phys. C **21**, 3585 (1988).
[16] Ma Dong-ping, Liu Yan-yun, Wang De-chao, and Chen Ju-rong, J. Phys.: Condens. Matter **7**, 4883 (1995).
[17] Ma Dong-ping, Zheng Xi-te, Xu Yi-sun, and Zhang Zheng-gang, Phys. Lett. A **115**, 245 (1986).
[18] Hong Hua, Sergey Mirov, and Yogesh Vohra, Phys. Rev. B **54**, 6200 (1996).
[19] R. D. Shannon, Acta Crystallogr., Sect. A: Cryst. Phys., Diffr., Theor. Gen. Crystallogr. **A32**, 751 (1976).
[20] Ma Dong-ping, Huang Xiao-yi, Chen Ju-rong, Zhang Ji-ping, and Zhang Zheng-gang, Phys. Rev. B **48**, 4302 (1993).
[21] Ma Dong-ping, Huang Xiao-yi, Chen Ju-rong, Liu Yan-yun, and Zhang Ji-ping, Phys. Rev. B **48**, 14 067 (1993).
[22] Ma Dong-ping, Liu Yan-yun, Ma Ning, and Chen Ju-rong, J. Phys. Chem. Solids **61**, 799 (2000).
[23] Ma Dong-ping, Chen Ju-rong, and Ma Ning, Commun. Theor. Phys. **36**, 357 (2001).
[24] Ma Dong-ping, Liu Yan-yun, Ma Ning, and Chen Ju-rong, Commun. Theor. Phys. **37**, 373 (2002).
[25] G. F. Imbusch, W. M. Yen, and A. L. Schawlow, Phys. Rev. **136**, A481 (1964).
[26] T. Kushida and M. Kikuchi, J. Phys. Soc. Jpn. **23**, 1333 (1967).
[27] B. Di Bartolo and R. C. Powell, *Phonons and Resonances in Solids* (John Wiley and Sons, New York, 1976).
[28] S. Sugano, Y. Tanabe, and H. Kamimura, *Multiplets of Transition-Metal Ions in Crystals* (Academic, New York, 1970).
[29] S. M. Healy, C. J. Donnelly, T. J. Glynn, G. F. Imbusch, and G. P. Morgan, J. Lumin. **44**, 65 (1989).
[30] A. Monteil, W. Nie, C. Madej, and G. Boulon, Opt. Quantum Electron. **22**, S247 (1990).
[31] S. M. Healy, C. J. Donnelly, T. J. Glynn, G. F. Imbusch, and G. P. Morgan, J. Lumin. **46**, 1 (1990).
[32] G. F. Imbusch, T. J. Glynn, and G. P. Morgan, J. Lumin. **45**, 63 (1990).
[33] J. B. Gruber, M. E. Hills, C. A. Morrison, G. A. Turner, and M. R. Kokta, Phys. Rev. B **37**, 8564 (1988).
[34] A. A. Kaminskii, *Laser Crystals (Their Physics and Properties)* (Springer-Verlag, Berlin, 1981), p. 320.
[35] K. P. O'Donnell, A. Marshall, M. Yamaga, B. Henderson, and B. Cockayne, J. Lumin. **42**, 365 (1989).
[36] B. Henderson and G. F. Imbusch, *Optical Spectroscopy of Inorganic Solids* (Oxford University Press, New York, 1989).
[37] B. Henderson, A. Marshall, M. Yamaga, K. P. O'Donnell, and B. Cockayne, J. Phys. C **21**, 6187 (1988).
[38] Ma Dong-ping, Ma Ning, Chen Ju-rong, and Lin Qiang, Commun. Theor. Phys. **33**, 167 (2000).
[39] Ma Dong-ping, Zhang Hong-mei, Chen Ju-rong, and Liu Yan-yun, Commun. Theor. Phys. **30**, 491 (1998).
[40] M. H. Crozier, Phys. Lett. **18**, 219 (1965).
[41] M. Yamaga, B. Henderson, A. Marshall, and K. P. O'Donnell, J. Lumin. **43**, 139 (1989).
[42] S. Geschwind, R. J. Collins, and A. L. Schawlow, Phys. Rev. Lett. **3**, 545 (1959).
[43] T. Muramoto, T. Fukuda, and T. Hashi, J. Phys. Soc. Jpn. **26**, 1551 (1969).
[44] Y. Tokura and N. Nagaosa, Science **288**, 462 (2000).